

## Article

# Mechanical Properties of Slag-Based Geopolymer Grouting Material for Homogenized Micro-Crack Crushing Technology

Wenjie Li <sup>1</sup>, Bin Liang <sup>1</sup> and Jinchao Yue <sup>2,\*</sup>

<sup>1</sup> School of Civil Engineering and Architecture, Henan University of Science and Technology, Luoyang 471000, China; liwenjie041@126.com (W.L.); liangbin4231@163.com (B.L.)

<sup>2</sup> Yellow River Laboratory, Zhengzhou University, Zhengzhou 450001, China

\* Correspondence: yuejc@zzu.edu.cn

**Abstract:** Homogenized micro-crack crushing can fully retain the bearing capacity of concrete pavement, but local weak road base needs to be reinforced before being directly overlaid with hot-mixed asphalt. Therefore, indoor tests were conducted to study the mechanical properties of slag-based geopolymer as a grouting material for weak road base, and the morphology and influence of polymerization reactants were observed. Concurrently, on-site grouting tests were conducted to study the grouting effect. The results show that the compressive strength, flexural strength and bonding strength of slag-based geopolymer all increase with age. The maximum compressive strength and flexural strength of the geopolymer at 28 d were 18.88 MPa and 6.50 MPa, respectively. The maximum flexural bonding strength at 14 d was 4.58 MPa. As the ratio between water and slag powder increased, the compressive strength and flexural strength gradually decreased, while the bonding strength first increased and then decreased. In the range of ratios of water to slag powder from 0.26 to 0.28, the above three strengths were relatively high, and the compressive shear bonding strength was the highest when the ratio of water to slag powder was 0.28. The shrinkage of the slag-based geopolymer increases with the increase in ratio of water to slag powder, and the porosity also increases, resulting in a decrease in compactness after consolidation. When the ratio of water to slag powder was 0.28, the reactant was mainly a gel-phase material, and the shrinkage crack of the consolidated geopolymer was relatively small. After grouting the weak road base of the concrete pavement, the voids at the bottom of the concrete pavement slab were effectively filled, and the deflection of the pavement slab was significantly reduced. The average deflections of monitoring line I, monitoring line II and monitoring line III decreased by 49%, 41% and 54%, respectively, after grouting. After solidification, the slag-based geopolymer was distributed in layers, which further compacted the road structure layer and improved the bearing capacity.

**Keywords:** concrete pavement; homogenized micro-crack crushing; slag-based geopolymer; mechanical properties; experimental investigations



**Citation:** Li, W.; Liang, B.; Yue, J. Mechanical Properties of Slag-Based Geopolymer Grouting Material for Homogenized Micro-Crack Crushing Technology. *Appl. Sci.* **2023**, *13*, 8353. <https://doi.org/10.3390/app13148353>

Academic Editors: José Neves and Tatsuya Ishikawa

Received: 8 June 2023

Revised: 14 July 2023

Accepted: 15 July 2023

Published: 19 July 2023



**Copyright:** © 2023 by the authors. Licensee MDPI, Basel, Switzerland. This article is an open access article distributed under the terms and conditions of the Creative Commons Attribution (CC BY) license (<https://creativecommons.org/licenses/by/4.0/>).

## 1. Introduction

Concrete pavement is one of the typical structural forms of high-grade highways at home and abroad. With the development of the economy, traffic flow gradually increases. When there are problems in design, construction and maintenance, concrete pavement suffers from various degrees of diseases such as corner breaks, cracks, depressions, pavement pumping and faulting of the slab ends, which seriously affect driving safety. A large amount of concrete pavement is in urgent need of rehabilitation. Compared to the old concrete pavement rehabilitation methods, homogenized micro-crack crushing is a novel concrete pavement rehabilitation technology. This method combines the advantages of multiple head breakers, impact compactors, guillotine breakers and resonant pavement breakers, making full use of the bearing capacity of the original pavement slab. However, some old concrete pavement rehabilitation techniques have problems such as insufficient

bearing capacity of the road base and insufficient strength of the concrete pavement slab. After homogenized micro-crack crushing of the pavement slab, the road base needs to be grouted to enhance the bearing capacity. Due to its excellent mechanical properties, early strength and rapid solidification characteristics, good volume stability and good impermeability, geopolymer materials have gradually become more used to reinforce the road base.

The term geopolymer was first coined by Davidovits to describe a three-dimensional network gel of aluminum oxide tetrahedron and silicon oxide tetrahedron prepared from solid waste, natural minerals, inorganic silicon aluminum compounds and other raw materials [1]. Due to the excellent mechanical properties of geopolymers, scholars at home and abroad have conducted extensive research on the preparation process and properties of geopolymers. Fernandez-Jimenez and Duxson [2,3] reviewed the history of geopolymer technology and established a descriptive model for the microstructural development of fly-ash-based cementitious geopolymers. Park and Kang [4] studied the effects of different activator concentrations, liquid/fly ash ratios, and curing temperatures and times on strength development in low-calcium fly ash geopolymer. Fernandez-Jimenez, Garcia-Lodeiro and Palomo [5] studied the durability, stability and microstructure changes in fly ash geopolymers in different environments. Ma, Hu and Ye [6] studied the development of the reaction degree, strength and compressive strength of fly ash geopolymer under activating solutions, and the results showed that the material had a denser microstructure. Nath and Kumar [7] studied the effect of slag addition to the geopolymerization reaction and consequent structural rearrangement, and found that GCS showed similar characteristics to GBFS, meaning it can be used as a substitute for GBFS in fly-ash-based geopolymer. Rashad [8] studied the effects of different admixtures and mineral admixtures on the performance of fly ash geopolymer, and the results showed that fly ash geopolymer had excellent characteristics and application prospects. Law et al. [9] compared the durability performance of Portland cement and fly ash geopolymer, and the results showed that when the concentration of the activator was relatively high, the durability of the geopolymer was better than that of cement. Khan et al. [10] evaluated the viability of developing a high-strength geopolymer composite by using low-calcium fly ash as a principal binder, as well as its partial replacement with slag, hydrated lime and ultra-fine fly ash in the mortar mixtures. Ding, Cheng and Dai [11] prepared geopolymer paste by using ground granulated blast furnace slag and coal fly ash and investigated the functional properties of geopolymer paste. Rakhimova and Rakhimov [12] reviewed the study of reaction products, structure and properties of alkali-activated metakaolin cements. Katpady et al. [13] studied the behavior of geopolymer under varied mixture proportions of ground granulated blast furnace slag and curing conditions. Guo and Pan [14] studied the effects of steel slag on the mechanical properties and microstructure of geopolymers. Ng et al. [15] presented the formulation and flexural properties of thin fly ash geopolymers and found that the flexural performance of thin geopolymers exhibited comparatively similar flexural strengths but a higher strength/thickness ratio compared to geopolymers with thickness greater than 40 mm. Stankiewicz [16] conducted research on effects of different admixtures on the properties of fly-ash-based geopolymer composites.

Many scholars have conducted extensive research on the preparation of geopolymers in which the main raw materials include fly ash, metakaolin, silica fume and slag. Research on the reaction products, strength and microstructure of materials is relatively detailed, mainly focusing on the reaction mechanism, structural properties and applications of geopolymers. Due to their high early strength, good durability, volume stability and high interfacial bonding strength, geopolymers are also suitable for road repair and reinforcement. Wang et al. [17] prepared road alkali-activated blast furnace slag (AABFS) paste which could be applied effectively in road-grouting reinforcement. Using Fullerfine sand powders (Fuller-FS) as a fine inorganic admixture, Xiang et al. [18] conducted research on effects of this addition on rheological properties, drying shrinkage and mechanical strength of MGGMs. Liu et al. [19] developed a new kind of powder geopolymer grouting

material (S-F powder Geopolymer) and investigated the properties. Xu et al. [20] investigated the workability, mechanical properties and microstructure of geopolymer grouting material (GGM) containing high-calcium basalt fiber (HCBF). Xu et al. [21] developed a high-performance geopolymer grouting material based on slag and fly ash and investigated the properties. Zhou et al. [22] prepared geopolymer road grouting pastes in different mixture ratios of volcanic ash (VA) and metakaolin (MK). Zeng et al. [23] experimentally investigated the effects of varying contents of Na<sub>2</sub>O in a modified sodium silicate, sodium silicate moduli (M-s), and the contents of granulated blast furnace slag (GBFS) on the compressive strength and drying shrinkage of fly-ash (FA)-based geopolymer grouting materials at different ages. Liu et al. [24] conducted an experimental investigation on the performance variation of geopolymer grouting material with varied mass fractions of raw materials and presented the optimal mix proportion. Yue et al. [25] prepared slag/fly-ash-based geopolymer materials for cement-stabilized macadam in road bases. Sofri et al. [26] explored the effects of FAG on road base layer properties using a mechanistic laboratory evaluation and its practicability in pavement base layers. Wu et al. [27] proposed a fly-ash-/slag-based geopolymer as an alternative to cement for stabilizing soft soils. Li et al. [28] conducted research on the mechanical properties of fly ash-slag-based geopolymer to solve various problems, such as difficulty to store and transport liquid activator of the existing geopolymer grouting materials.

In summary, some researchers focused on the preparation of geopolymers the main raw materials of which included fly ash, metakaolin, silica fume, and slag. Some studies also focused on the mechanical properties of geopolymers using them as grouting materials for conventional road maintenance methods. To the best of our knowledge, little work had been reported to address the mechanical properties and microscopic morphology of geopolymer which is used as a grouting material in homogenized micro-crack crushing technology. In this study, a slag-based geopolymer grouting material was prepared, which was used in concrete pavement rehabilitation after homogenized micro-crack crushing. Through indoor tests, the compressive strength, flexural strength, flexural bonding strength, and compressive shear bonding strength under different ratios of water to slag powder of geopolymer were studied. At the same time, the microstructure of geopolymer was observed using SEM and elemental composition of the corresponding polymerization reactants was analyzed. Furthermore, through on-site grouting tests, the grouting effect of slag-base geopolymer on the road base was studied after homogenized micro-crack crushing.

## 2. Experimental Section

### 2.1. Materials

The main raw material for slag-based geopolymer is blast furnace slag powder, which is a gray white powder. Referring to “Ground granulated blast furnace slag used for cement, mortar and concrete” (GB/T 18046-2017) [29], the density and the specific surface area of the slag powder were 2.93 g/cm<sup>3</sup> and 459 m<sup>2</sup>/kg. XRF was used to determine the chemical composition, and the main components are presented in Table 1. The main components of slag included silicon oxide, calcium oxide, aluminum oxide, and magnesium oxide, with a relatively low content of other components.

**Table 1.** Chemical composition of raw materials (wt.%).

Material	CaO	SiO <sub>2</sub>	Al <sub>2</sub> O <sub>3</sub>	MgO	SO <sub>3</sub>	TiO <sub>2</sub>	Fe <sub>x</sub> O <sub>y</sub>	Na <sub>2</sub> O	K <sub>2</sub> O	MnO
slag	39.46	26.01	13.24	8.41	2.25	1.04	0.68	0.60	0.60	0.30

The crystal structure of blast furnace slag powder was analyzed using XRD (X-ray diffraction), and the XRD patterns of blast furnace slag powder are shown in Figure 1. The crystallinity of blast furnace slag powder was slightly poor, with weak diffraction peaks and more impurity peaks. When the diffraction angle was about 30°, a diffuse diffraction peak area appeared, which indicated that the main structure of the raw material

was amorphous. It indicated the presence of a large amount of glass phase composition and almost an absence of a complete crystal phase. The micro powder of blast furnace slag was rich in  $\text{Al}_6\text{Si}_2\text{O}_{13}$  and  $\text{SiO}_2$ , which were the main sources of potential activity in the glass phase structure and the main components of polymerization reactions.

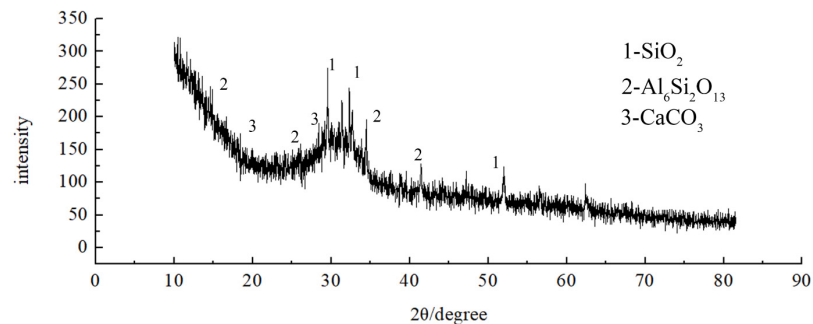


**Figure 1.** XRD patterns of blast furnace slag powder.

## 2.2. Preparation of Geopolymer

The geopolymer was prepared with slag powder and alkaline activator, and the alkali activator was prepared with sodium silicate and sodium hydroxide with a mass ratio of 10.1:1. During the preparation of the geopolymer, the slag powder and the alkaline activator were mixed and stirred slowly with a mixer for 2 min; after about 10 s, the mixture was quickly stirred for 2 min again. Then, the mixed slurry was molded and compacted on a vibration table. Finally, the specimen was placed in a standard curing room. Under a certain amount of alkaline activator, five ratios of water to slag powder of 0.24, 0.26, 0.28, 0.30, and 0.32 were selected to study the mechanical properties of the geopolymer. Referring to “Testing Methods of Cement and Concrete for Highway Engineering” (JTG 3420-2020) [30], compressive strength, flexural strength, and bonding strength of the geopolymer were tested.

## 2.3. Testing Methods

### 2.3.1. Compressive and Flexural Strength Tests

The specimen size of the compressive strength test was  $\Phi 50 \text{ mm} \times 50 \text{ mm}$ , while that of the flexural strength test was  $40 \times 40 \times 160 \text{ mm}^3$ . According to the standard curing condition in “Testing Methods of Cement and Concrete for Highway Engineering” (JTG 3420-2020) [30], compressive and flexural strengths of the specimens were tested at 3 d, 7 d, and 28 d under 5 different ratios of water to slag powder. The specimens of compressive strength test and flexural strength test are shown in Figure 2.



**Figure 2.** The specimens of the compressive strength and the flexural strength tests. (a) The specimens of compressive strength test; (b) The specimens of flexural strength test.



### 2.3.2. Bonding Strength Test

There are two test methods for the bonding strength of a geopolymer. One is flexural strength test of the new and the old bonding beam, and the other is the compressive shear bonding strength test. In the new and the old bonding beam flexural strength tests, the cement mortar specimens were first poured, and the flexural strength was tested at 3 d, 7 d, and 14 d. Then, based on half of the cement mortar beam inside the mold, the geopolymer slurry was poured again, and the flexural strength of the specimens at 3 d, 7 d, and 14 d was tested. The poured specimens and the flexural strength test are shown in Figure 3. In the compressive shear bond strength test, a rectangular concrete block was first designed as a mold which had a cylindrical hole at the center. The thickness of the mold was 50 mm, and there were three types of cylindrical hole diameters, 52 mm, 57 mm, and 62 mm. The geopolymer slurry was poured into the cylindrical hole, and then load was applied at the center of specimen to test the compressive shear bonding strength at 3 d, 7 d, and 28 d, respectively. The specimens and the compressive shear bonding strength test are shown in Figure 4.

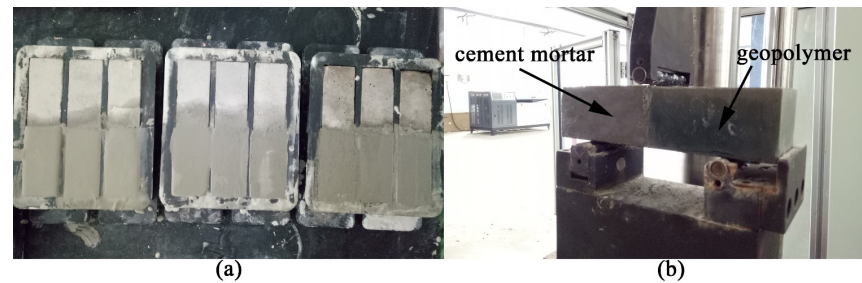


**Figure 3.** New and old bonding beams and the flexural strength test. (a) New and old bonding beams; (b) Flexural strength test.

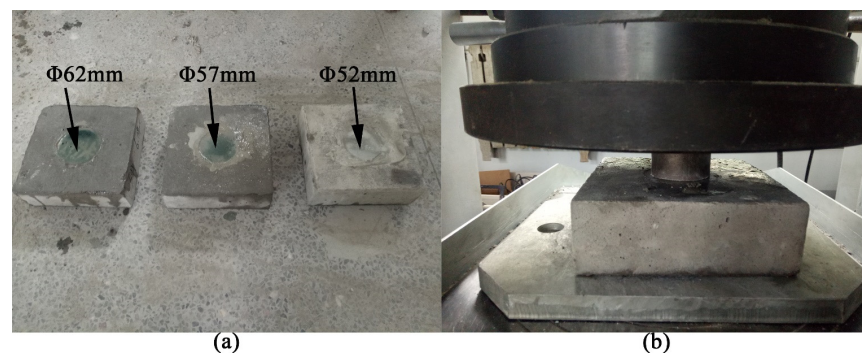


**Figure 4.** Three types of specimens and compressive shear bonding strength test. (a) Three types of specimens; (b) Compressive shear bonding strength test.

### 2.3.3. Microscopic Test

The reaction products, the pore structure and the gel of the slag-based geopolymer were observed by SEM, and the KYKY-EM6200 scanning electron microscope (SEM) was used. The scanning electron microscope was equipped with an X-ray energy dispersive spectrometer (EDS), which could observe the micro zone composition and conduct qualitative and quantitative analysis of the elemental composition of the geopolymer.

## 3. Results and Discussion

### 3.1. Compressive Strength of Geopolymer

The compressive strength of the five ratios of water to slag powder of 0.24, 0.26, 0.28, 0.30, and 0.32 at different ages of 3 d, 7 d, and 28 d is shown in Figure 5. As shown in Figure 5a, when the ratio of water to slag powder increased, the compressive strength of geopolymer gradually decreased. The geopolymer with a ratio of water to slag powder of

0.24 had the highest compressive strength, with strengths of 12.56 MPa, 16.22 MPa, and 18.88 MPa at 3 d, 7 d, and 28 d, respectively. However, the compressive strength of the geopolymer with a ratio of water to slag powder of 0.32 was the smallest, with strengths of 8.38 MPa, 12.26 MPa, and 16.46 MPa at the age of 3 d, 7 d, and 28 d, respectively. As shown in Figure 5b, due to the characteristic of early strength and rapid solidification of the geopolymer, the compressive strength grew the fastest within 1 to 3 days, followed by the growth rate of 3 to 7 days. The strength of geopolymer with a ratio of water to slag powder of 0.24 increased the fastest, reaching 67% of the 28 d strength at 3 d and 86% of the 28 d strength at 7 d, followed by a geopolymer with a ratio of water to slag powder of 0.28, the strength at 3 d and 7 d being 56% and 82% of the 28 d strength, respectively.

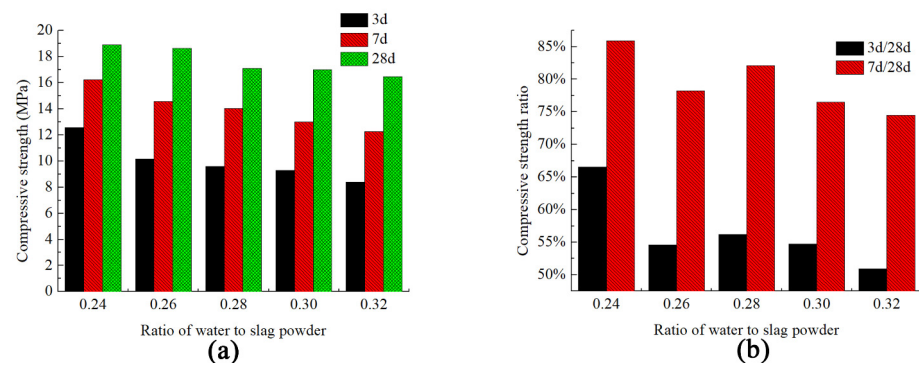


**Figure 5.** Compressive strength and ratio of geopolymer at different ratios of water to slag powder. (a) Compressive strength; (b) Compressive strength ratio.

### 3.2. Flexural Strength of Geopolymer

The flexural strength of the five ratios of water and slag powder of 0.24, 0.26, 0.28, 0.30, and 0.32 at different ages is shown in Figure 6. As shown in Figure 6a, as the ratio of water to slag powder increased, the flexural strength of the geopolymer gradually decreased, with the maximum reduction in flexural strength at 28 d. The geopolymer with a ratio of water to slag powder of 0.24 had the highest flexural strength, with strengths of 2.70 MPa, 3.60 MPa, and 6.50 MPa at 3 d, 7 d, and 28 d, respectively. However, when the ratio of water to slag powder was 0.32, the flexural strength was the smallest, with strengths of 1.93 MPa, 2.73 MPa, and 4.10 MPa for the three ages, respectively. As shown in Figure 6b, the growth rate of flexural strength was the fastest within 1 to 3 days; it gradually slowed down within 3 to 7 days. The flexural strength of the geopolymer with a ratio of water to slag powder of 0.32 had the highest growth rate in 1~3 d and 3~7 d, the strength ratios of 3 d to 28 d and 7 d to 28 d were 47% and 67%. The other ratios of water to slag powder with faster growth rates of flexural strength were 0.26 and 0.28, respectively.

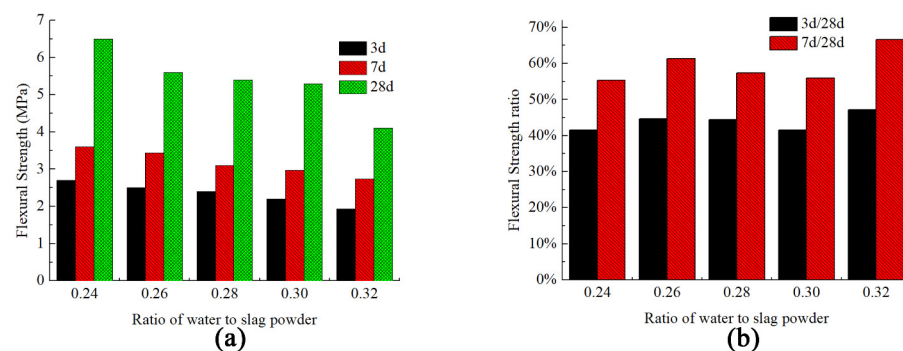


**Figure 6.** Flexural strength and ratio of geopolymer at different ratios of water to slag powder. (a) Flexural Strength; (b) Flexural Strength ratio.

As a road grouting material, geopolymers could fill the void of the road and reinforce the road base, requiring good mechanical properties. Under traffic loads, the geopolymer should have not only a certain compressive and flexural strength, but also a certain degree of flexibility. The ratio of compressive strength to flexural strength of the geopolymer reflected the brittleness of the material. The higher the ratio, the greater the brittleness of the geopolymer. If the ratio is opposite, the flexibility of the geopolymer is better. In order to reflect the flexibility of the geopolymer, the ratio of compressive strength to flexural strength was used. The compressive and flexural strength ratio of the five ratios of water to slag powder of the geopolymer at different ages of 3 d, 7 d, and 28 d are shown in Figure 7. As shown in Figure 7, the compressive–flexural ratio of the five ratios of water to slag powder of geopolymer mostly increased and then decreased with age. The main reason was that the growth rate of the 7 d geopolymer compressive strength was significantly higher than that of the 7 d flexural strength. The 3 d compressive–flexural ratio of the water to slag powder ratio of 0.28 geopolymer was the smallest, while the 28 d compressive–flexural ratio of the water to slag powder ratio of 0.24 geopolymer was the smallest. However, the 28 d compressive–flexural ratio of the water to slag powder ratio of 0.28 geopolymer was only slightly higher than that of the water to slag powder ratio of 0.24. The geopolymer belonged to the early strength type, and the growth rate of early strength was relatively fast. When it was used to reinforce the road base, it required not only high compressive strength and flexural strength, but also good flexibility. From the analysis of compressive strength, flexural strength, and compressive–flexural ratio, it can be seen that the geopolymer with a ratio of water to slag powder of 0.28 had better mechanical properties.

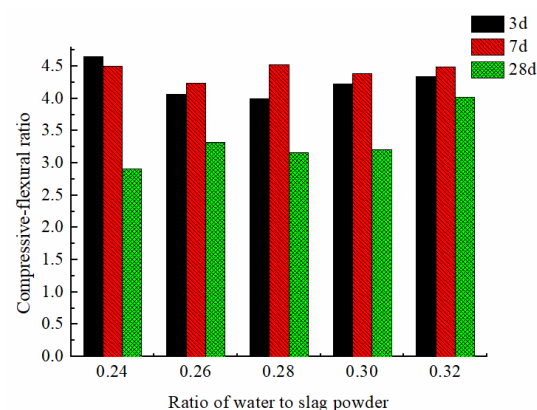


**Figure 7.** Compressive–flexural ratio.

### 3.3. Flexural Strength of New and Old Bonding Beams

Geopolymer was used as a grouting material to reinforce concrete pavement, fill the void of the road base, and also bond and solidify loose particles. Bonding strength was a mechanical indicator that reflected the adhesion between geopolymer materials and road base, but there was no unified test method yet. The bonding strength of geopolymer materials was studied using new and old bonding beam flexural strength test methods, and the basic principle of the test was based on “Testing Methods of Cement and Concrete for Highway Engineering” (JTG 3420-2020) [30]. The flexural strength tests were conducted at the age of 3 d, 7 d, and 14 d, and the failure surface of new and old bonding beams are shown in Figure 8. At the age of 3 d, the flexural failure surfaces of new and old bonding beams were on the side of the geopolymer. As the age increased, the flexural strength of the geopolymer increased rapidly. Therefore, at the age of 7 d, the failure surfaces of new and old bonding beams were close to the bonding surface, and the failure surfaces exposed both the geopolymer and the cement mortar. At the age of 14 d, the failure surface of the specimen almost simultaneously passed through the geopolymer and the cement mortar beam.

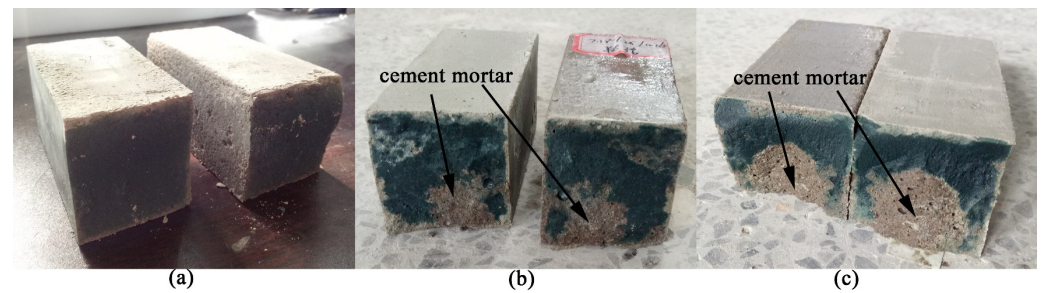


**Figure 8.** Failure surface of new and old bonding beams. (a) 3 d; (b) 7 d; (c) 14 d.

The flexural strength of new and old bonding beams with the five types of ratios of water to slag powder, including 0.24, 0.26, 0.28, 0.30, and 0.32, is shown in Figure 9. As shown in Figure 9a, when age increased, the flexural strength of new and old bonding beams gradually increased. However, with the increase in the ratio of water to slag powder, the overall flexural strength showed a trend of first increasing and then decreasing under the same age. As shown in Figure 9b, when the age was 3 d, the flexural strength of the new and old bonding beams could reach 48% to 63% of the values of the mortar beams. When the ages were 7 d and 14 d, the flexural strengths of the new and old bonding beams could reach 72% to 94% and 80% to 97% of the values of the original mortar beams, respectively. The data showed that the bonding flexural strength of the geopolymer slurries with ratios of water to slag powder of 0.26 and 0.28 was better. The polymerization reactants of the geopolymer slurry could adhere to the mortar interface to prevent the expansion of microcracks, thereby improving the flexural strength of new and old bonding beams. At the same time, due to the filling effect of the geopolymer in the large pores of the mortar, the microporous connection hole was blocked, which enhances the bonding effect between the geopolymer beam and the mortar beam.

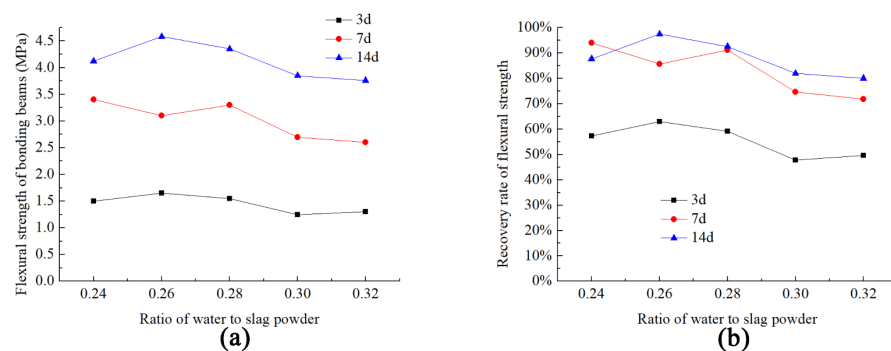


**Figure 9.** Flexural strength of bonding beam and recovery rate of flexural strength. (a) Flexural strength of bonding beams; (b) Recovery rate of flexural strength.

### 3.4. Compressive Shear Bonding Strength

During the compressive shear bonding strength tests, when there was shear dislocation between the rectangular concrete block and the geopolymer cylindrical core, their bonding was considered to be a failure. The compressive shear bonding strength under the five ratios of water to slag powder of 0.24, 0.26, 0.28, 0.30, and 0.32 at different ages of 3 d, 7 d, and 28 d is shown in Figure 10. Under different ages of 3 d, 7 d, and 28 d, as the ratio of water to slag powder increased, the compressive shear bonding strength showed a trend of first increasing and then decreasing. The compressive shear bonding strength reached its maximum at the ratio of water to slag powder of 0.28. As the age increased, the compressive shear bonding strength of the  $\Phi$  52 mm,  $\Phi$  57 mm, and  $\Phi$  62 mm types of geopolymer cylindrical core showed a decreasing trend. The reason was that the slag geopolymer had a certain degree of shrinkage with the increase in age, which would affect the bonding performance of the material. When the age was 28 d, the difference in compressive shear



bonding strength among the three diameter geopolymer cylindrical core was small, and the changes in compressive shear bonding strength of the five ratios of water and slag powder were also not significant.

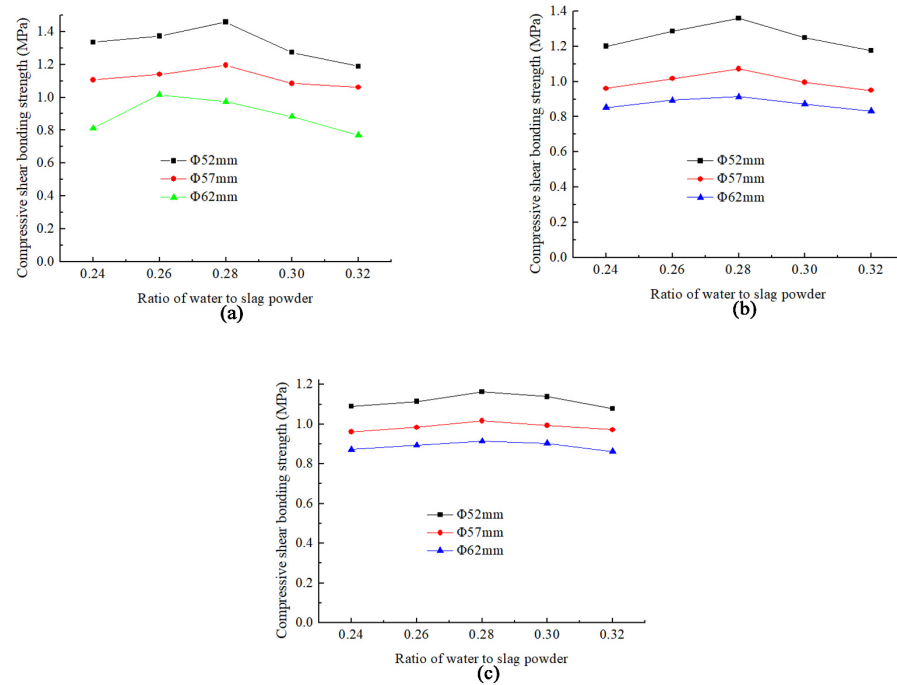


**Figure 10.** Compressive shear strengths of geopolymer at different ages. (a) Compressive shear bonding strength of 3 d age; (b) Compressive shear bonding strength of 7 d age; (c) Compressive shear bonding strength of 28 d age.

In order to analyze the effect of shrinkage of the geopolymer on the compressive shear bonding strength, the average of the five ratios of water to slag powder at the same age was calculated, and the variation in compressive shear bonding strength is shown in Figure 11. The compressive shear bonding strength of the geopolymer cylindrical core of Φ 62 mm was the smallest, and the strength of the three ages was relatively similar. This was because the bonding area of the geopolymer cylindrical core was the largest, resulting in a large shrinkage and a smaller bonding strength. As the bonding area of the Φ 57 mm and Φ 52 mm geopolymer cylindrical core decreased, the shrinkage effect of the material decreased, resulting in an increase in bonding strength.

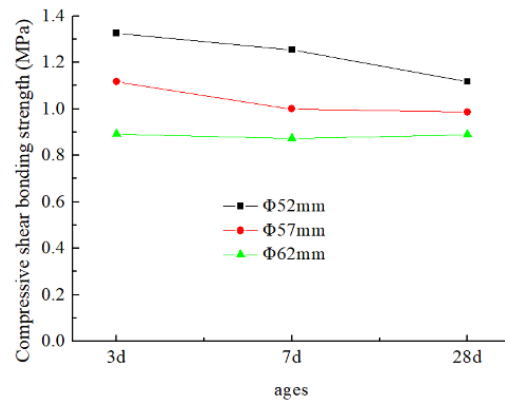


**Figure 11.** The effect of shrinkage of geopolymer at different ages on bonding strength.

Compared with flexural strength of new and old bonding beams, the trend of compressive shear bonding strength with the change in ratio of water and slag powder was

basically the same. However, due to the cylindrical shape of the geopolymer core, the shrinkage of the core affects the bonding between the geopolymer material and the concrete block. Therefore, the compressive shear bonding strength decreased with age. When the geopolymer was used for road grouting and base reinforcement, it was mainly used to bond loose particles and fill voids, which corresponds to the flexural strength of new and old bonding beam tests and compressive shear bonding strength tests. However, the voids in the road base were usually small, so the shrinkage of the geopolymer had a relatively small impact on the bonding strength.

### 3.5. Microscopic Test

The SEM images of the geopolymer under different ratios of water to slag powder at 28 d are shown in Figures 12–14. As shown in Figure 12, at a  $100\times$  magnification, when the ratio of water to slag powder was small, the surface of the geopolymer was dense. The alkali activator promoted the hydration process of the glass phase material in the slag geopolymer, resulting in a large number of gel particles arranged closely, so the material structure in the SEM images had small pores. When the ratio of water to slag powder increased, the increase in water content promoted the hydration and dissolution reaction of the slag in the early stage of reaction, but the pore size of the structure increased, resulting in a decrease in the density of the geopolymer. The SEM images of the material at a  $500\times$  magnification are shown in Figure 13. The image shows that as the water content increased, the shrinkage of the geopolymer material also increased, and the number and width of microcracks gradually increased.

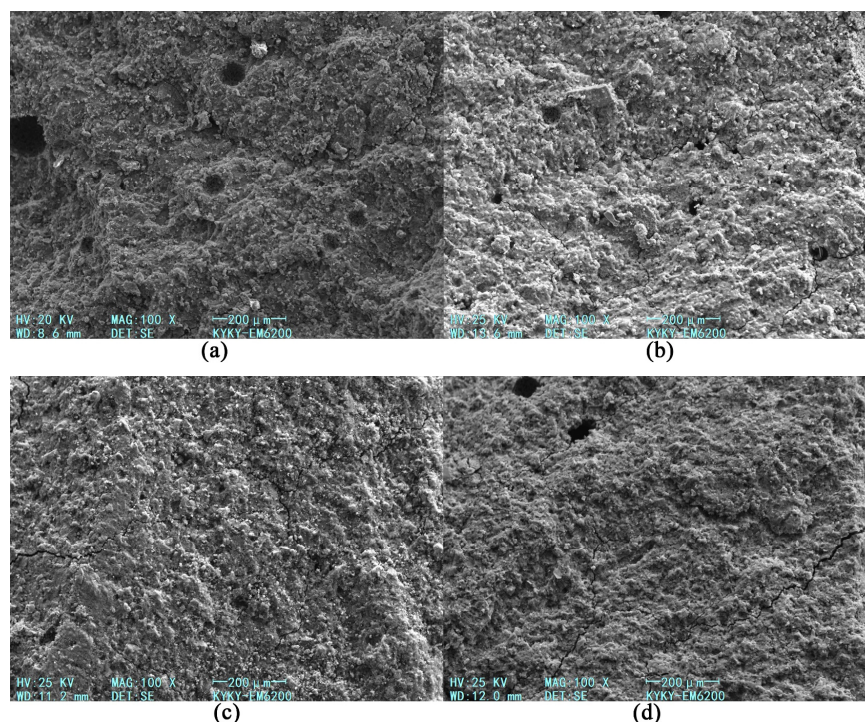


**Figure 12.** SEM images of geopolymer at different ratios of water to slag powder ( $200\ \mu\text{m}$ ). (a) Ratio of water to slag powder 0.24; (b) Ratio of water to slag powder 0.26; (c) Ratio of water to slag powder 0.28; (d) Ratio of water to slag powder 0.30.

As shown in Figure 14, at a  $2000\times$  magnification, when the ratio of water to slag powder was 0.24, there was a large number of flake calcium hydroxide crystals and granular geopolymer gels on the surface. As the ratio of water to slag powder gradually increased, the flake sodium hydroxide crystal gradually decreased. The main reaction product of the geopolymer with the ratio of water to slag powder of 0.28 and 0.30 was gel material. Due to the corresponding increase in the shrinkage reaction of the geopolymer, the structural

density decreased; moreover, the ratio of the water to slag powder of 0.30 cause the geopolymer material to have a lower density.

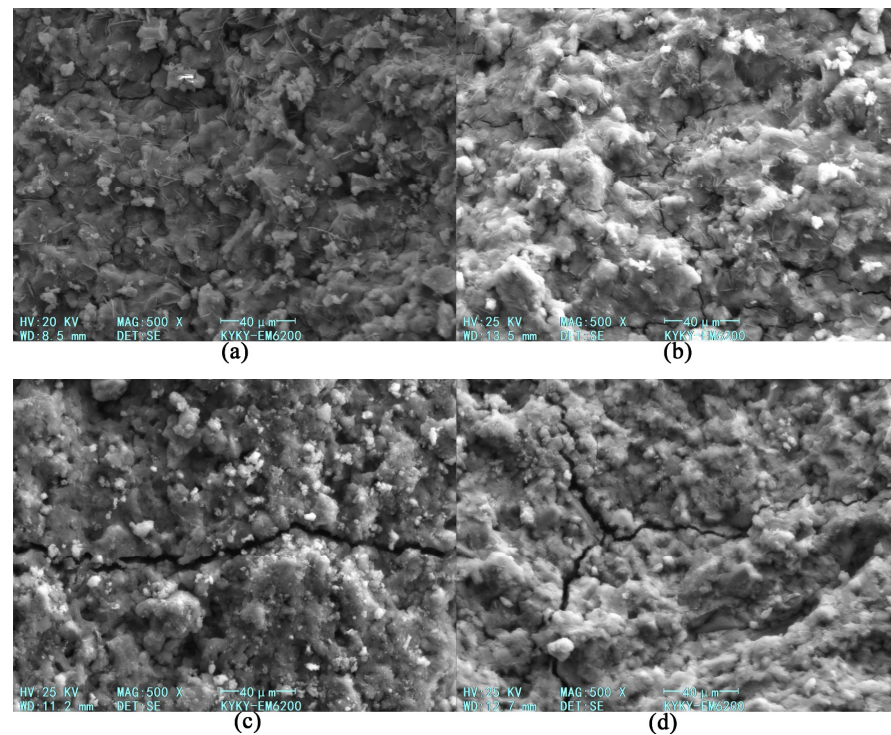


**Figure 13.** SEM images of geopolymer at different ratios of water to slag powder (40 μm). (a) Ratio of water to slag powder 0.24; (b) Ratio of water to slag powder 0.26; (c) Ratio of water to slag powder 0.28; (d) Ratio of water to slag powder 0.30.

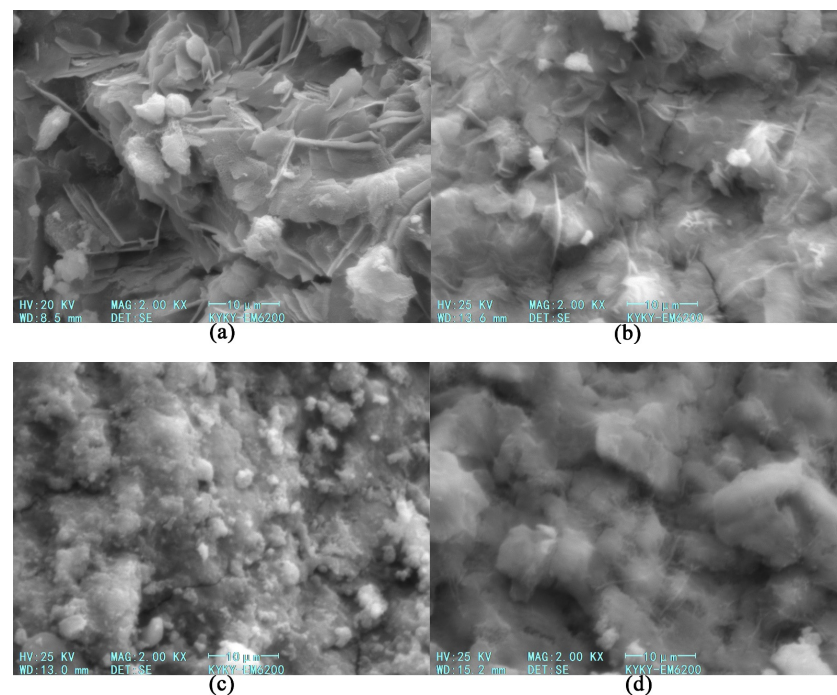


**Figure 14.** SEM images of geopolymer at different ratios of water to slag powder (10 μm). (a) Ratio of water to slag powder 0.24; (b) Ratio of water to slag powder 0.26; (c) Ratio of water to slag powder 0.28; (d) Ratio of water to slag powder 0.30.



In order to study the morphology of geopolymer reaction products, EDS analysis was conducted on micro regions of a 28 d geopolymer under the five ratios of water to slag powder. The SEM images and EDS spectra of micro regions with ratios of water to slag powder of 0.26, 0.28, and 0.30 under a  $2000\times$  magnification are shown in Figures 15–17. It could be seen from the SEM image that many gels was generated in the slag geopolymer, and the main product was the C-S-H gel. There were micro cracks on the surface of the slag geopolymer, and as the ratio of water to slag powder increased, the shrinkage of the geopolymer increased. Due to a decrease in the density of the geopolymer, the degree of surface porosity increased. According to the EDS spectrum, the main elements in the hydration products of slag-based geopolymer included Ca, Si, Al, Na, Mg, C, O, etc. Due to the existence of the Al element, some Si element in the C-S-H gel was replaced to form the C-A-S-H gel.

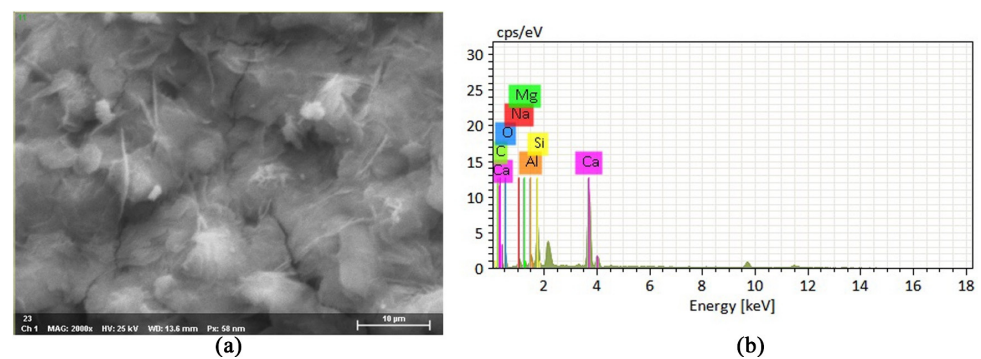


**Figure 15.** SEM image and EDS spectra of geopolymer with a ratio of water to slag powder of 0.26. (a) SEM image of ratio of water to slag powder 0.26; (b) Energy spectrum of ratio of water to slag powder 0.26.

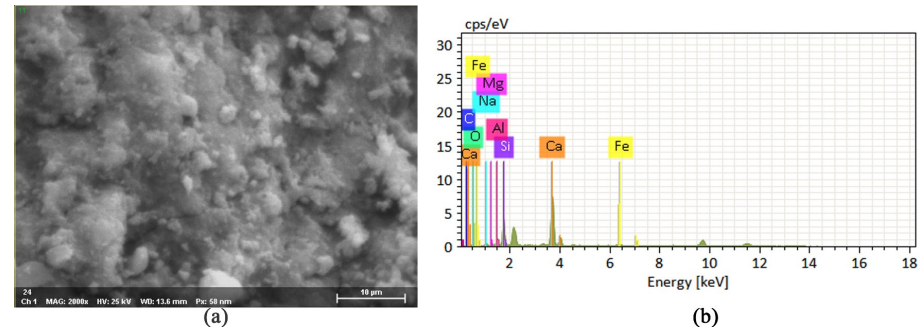


**Figure 16.** SEM image and EDS spectra of geopolymer with a ratio of water to slag powder of 0.28. (a) SEM image of ratio of water to slag powder 0.28; (b) Energy spectrum of ratio of water to slag powder 0.28.

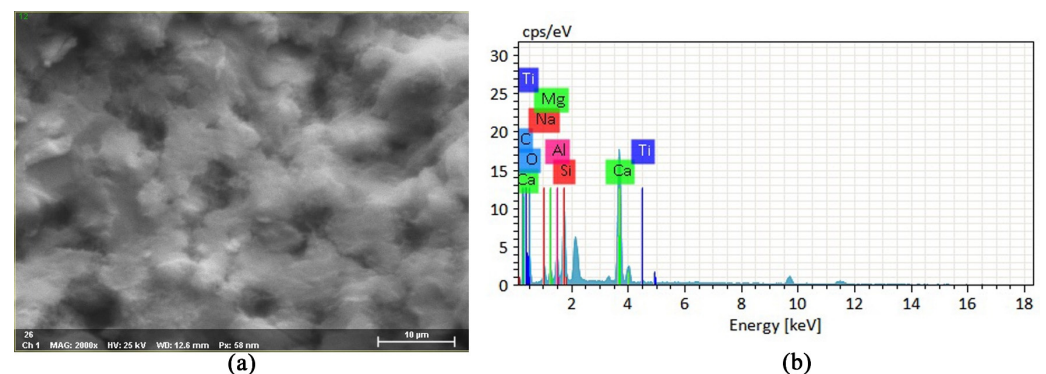


**Figure 17.** SEM image and EDS spectra of geopolymer with a ratio of water to slag powder of 0.30. (a) SEM image of ratio of water to slag powder 0.30; (b) Energy spectrum of ratio of water to slag powder 0.30.



The mass percentages of the main elements in the polymerization reactants with the five ratios of water to slag powder are shown in Figure 18. As the ratio of water to slag powder increased, the mass fractions of various elements showed a decreasing trend overall, mainly due to the dilution effect caused by increasing the water volume. Under the action of alkaline activator, the increase in water would accelerate the hydration of glass substances in a slag-based geopolymer powder, accelerating the reaction. However, due to the dilution of water in the late reaction period, the production of gel would be affected. Therefore, the larger the ratio of water to slag powder, the looser the structure, which has a certain impact on the macro physical and mechanical properties of a slag-based geopolymer.

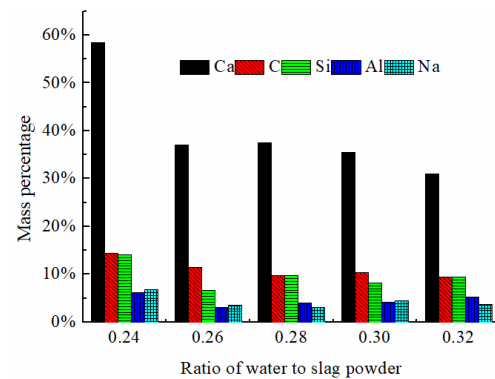


**Figure 18.** Mass percentage of geopolymer elements with different ratios of water to slag powder.

## 4. Practical Application

### 4.1. Homogenized Micro-Crack Crushing

When the concrete pavement was rehabilitated with homogenized micro-crack crushing technology, the bearing capacity of each structural layer of the road could be fully utilized so that the rehabilitated pavement could be directly overlaid with hot-mixed asphalt concrete. In homogenized micro-crack crushing technology, specialized mechanical equipment was used to impact the concrete pavement slab, in which the drop hammer was lifted to a predetermined height and then freely dropped to impact the concrete pavement slab. The bottom of the drop hammer was equipped with multiple impact heads, and after the concrete pavement slab was impacted, the impact position formed a compression shear fracture zone. The homogenized micro-crack crushing of the pavement slab is shown in Figure 19. After homogenized micro-crack crushing, the concrete pavement slab was broken into smaller pieces, and micro cracks were evenly distributed on the concrete pavement slab. The main cracks developed along the longitudinal direction of the impact head, while the branch cracks developed along the transverse direction of the impact head. When the impact head approached the edge of smaller pieces of the concrete pavement, branch cracks developed to the edge of the plate. When the impact head was far from the edge of the smaller pieces, the development of branch cracks was limited.

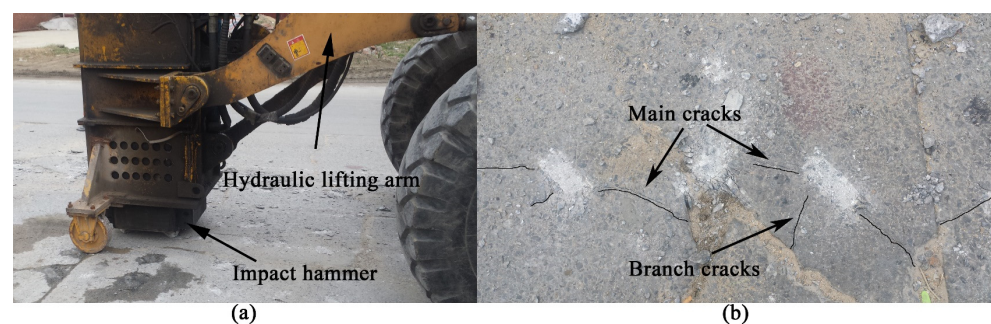


**Figure 19.** The homogenized micro-crack crushing of concrete pavement slab. (a) Impact crushing equipment; (b) Homogenized micro-crack crushing cracks.

#### 4.2. Practical Grouting Test of Geopolymer

Due to problems such as insufficient base bearing capacity and insufficient strength of concrete pavement in some of the rehabilitated areas, it was necessary to reinforce the road base through grouting after homogenized micro-crack crushing. The ratio of water to slag powder of the slag-based geopolymer prepared on site was 0.28. In the field grouting test, the hole was drilled manually, and the holes were arranged in a plum style. After the hole was formed, the PVC flower tube was placed in the hole so that the slurry was diffused in a directional manner and the weak road base around the hole was strengthened. During the grouting process, the amount of grouting was artificially controlled. When the adjacent grouting hole emitted slurry or the pavement slab raised, grouting was stopped. After the completion of geopolymer grouting, traffic was opened after a short period of curing, and then the hot mixed asphalt was overlaid. In order to verify the effectiveness of geopolymer grouting, the deflection of the concrete pavement slab before and after grouting was measured. Each monitoring line was 10 m long and the spacing between measuring points was 1 m. A half-width concrete pavement was selected, and three deflection monitoring lines with a spacing of 2 m were set up. The on-site deflection monitoring lines are shown in Figure 20.

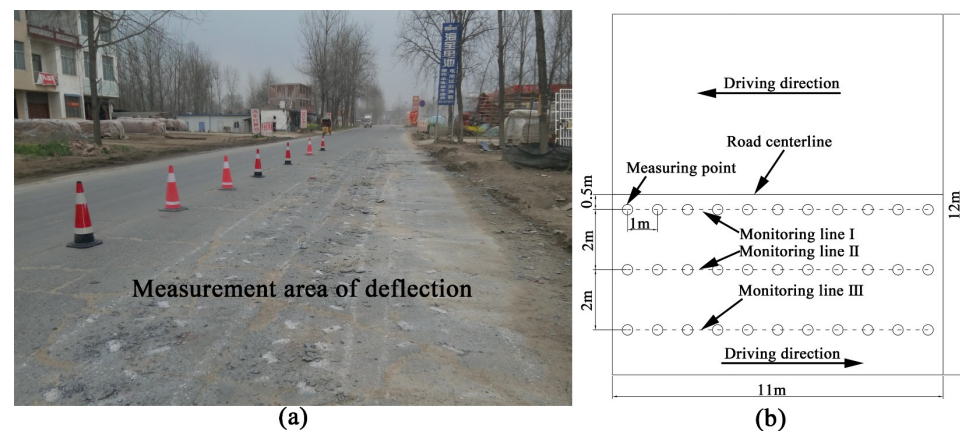


**Figure 20.** The deflection monitoring of pavement slab before and after grouting. (a) Measurement area of deflection on site; (b) Deflection measuring lines.

In the weak road base areas of concrete pavement, due to the void of concrete pavement slab and the weak road base, the deflection was large and some of the deflection was abnormal. The deflection of the concrete pavement slab before and after grouting is shown in Figure 21. After grouting at the diseased location of the pavement, the overall deflection significantly decreased, and the abnormal points of deflection were eliminated. The average deflection of monitoring line I, monitoring line II, and monitoring line III decreased from 88.2 (0.001 mm), 73.9 (0.001 mm), and 104.8 (0.001 mm) to 45.2 (0.001 mm), 43.9 (0.001 mm), and 48 (0.001 mm), respectively. The average deflection of monitoring line I, monitoring line II, and monitoring line III decreased by 49%, 41%, and 54%, respectively, after grouting. Moreover, the coefficient of variation of deflection values decreased by an average of 16%. After the consolidation of the geopolymer slurry, the void was filled, and the loose road base was consolidated, thereby the weak road base was reinforced and the deflection of the concrete pavement was reduced.

In order to observe the grouting effect of the geopolymer, typical disease locations were selected for excavation within the three monitoring line areas, as shown in Figure 22. After removing the concrete pavement slab through excavation, there was a layer of 5 mm geopolymer slurry consolidation between concrete pavement slab and cement stabilized base. Through excavation, it was found that geopolymer slurry effectively filled the void at the bottom of concrete pavement slab and the interlayer gaps between various structural layers of road. For loose road structural layers, the geopolymer slurry could consolidate

well. After solidification, the geopolymer slurry formed a layered structure, which was further compacted into the road structure layers; therefore, the overall bearing capacity of the road structure layers were improved.

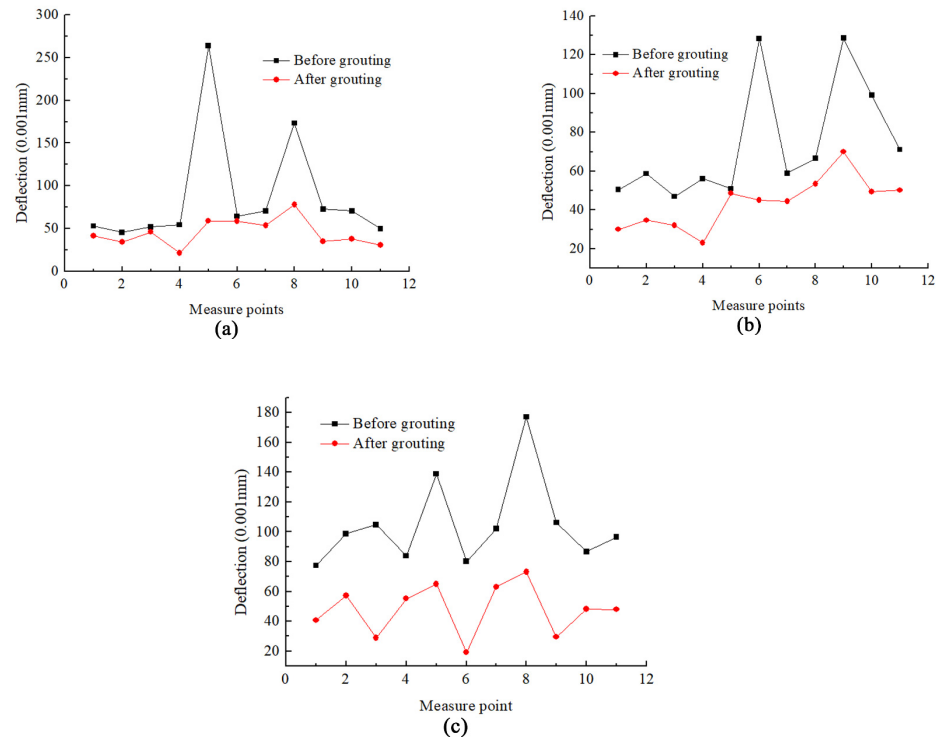


**Figure 21.** Deflection of the concrete pavement before and after grouting. (a) Deflection of monitoring line I; (b) Deflection of monitoring line II; (c) Deflection of monitoring line III.

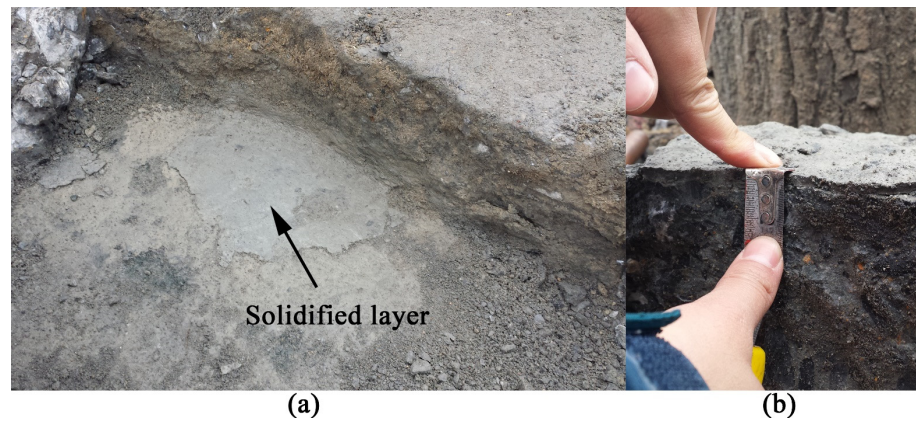


**Figure 22.** Grouting layer at the bottom of concrete pavement slab. (a) Solidified layer of geopolymer; (b) Layer thickness.

### 5. Conclusions

In this paper, indoor tests were conducted on the compressive strength, flexural strength, bonding strength of slag-based geopolymer grouting material used in homogenized micro-crack crushing technology, and the morphology and polymerization reactants of the geopolymer were observed. Moreover, on-site grouting tests were conducted to study the grouting effect of the geopolymer on the local weak road base. The main conclusions are presented below.

As the age increased, the compressive and flexural strength of the slag-based geopolymer gradually increased. The maximum compressive strength and the flexural strength of

the geopolymer at 28 d were 18.88 MPa and 6.50 MPa, respectively. The maximum flexural bonding strength at 14 d was 4.58 MPa. However, the compressive and flexural strength gradually decreased with the increase in the ratio of water to slag powder. The early strength of the geopolymer with a ratio of water to slag powder of 0.26 to 0.28 increased rapidly, among which the compressive and the flexural strengths of geopolymer materials with a ratio of water to slag powder of 0.28 were both better.

The flexural strength test of new and old bonding beams and the compressive shear bonding strength test methods were proposed. As the age increased, the bonding strength of the geopolymer gradually increased. However, as the ratio of water to slag powder increased, the bonding strength first increased and then decreased. The bonding performance of the geopolymer in the range of ratio of water to slag powder of 0.26~0.28 was good; specifically, the geopolymer with a ratio of water to slag powder of 0.28 had the highest compressive shear bonding strength.

Blast furnace slag powder was rich in CaO and SiO<sub>2</sub>, which could produce the C-S-H gel in geopolymer materials under the action of an alkali activator. As the ratio of water to slag powder increased, the shrinkage of the geopolymer slurry increased, the porosity increased, and the compactness decreased after consolidation. When the ratio of water to slag powder was small, a variety of crystal phase substances and gel phase substances coexisted. When the ratio of water to slag powder was 0.28, the reactants were mainly gel phase substances, and the shrinkage cracks were relatively small.

The slag-based geopolymer grouting material could effectively fill the voids at the bottom of the concrete pavement slab and also consolidate the loose material of the local road base. The average deflection of monitoring lines I, II, III decreased by 49%, 41%, and 54%, respectively, after grouting, and the coefficient of variation of deflection values decreased by an average of 16%. After the solidification of the geopolymer slurry, it was distributed in a layered manner, which further compacted the road structure layer and improved the overall bearing capacity of the road structure layer.

**Author Contributions:** Conceptualization, W.L. and J.Y.; methodology, J.Y.; software, W.L.; validation, W.L. and J.Y.; formal analysis, W.L.; investigation, J.Y.; resources, B.L.; data curation, W.L.; writing—original draft preparation, W.L.; writing—review and editing, J.Y.; visualization, W.L.; supervision, W.L.; project administration, B.L.; funding acquisition, B.L. All authors have read and agreed to the published version of the manuscript.

**Funding:** This research was funded by the Project of Science and Technology of Henan Transportation Department (Grant numbers 2018J4 and 2019J1).

**Institutional Review Board Statement:** Not applicable.

**Informed Consent Statement:** Not applicable.

**Data Availability Statement:** Not applicable.

**Conflicts of Interest:** The authors declare no conflict of interest.

## References

1. Davidovits, J. Geopolymers: Inorganic polymer new materials. *J. Therm. Anal.* **1991**, *37*, 1633–1656. [[CrossRef](#)]
2. Duxson, P.; Fernández-Jiménez, A.; Provis, J.L.; Lukey, G.C.; Palomo, A.; van Deventer, J.S. Geopolymer technology: The current state of the art. *J. Mater. Sci.* **2007**, *42*, 2917–2933. [[CrossRef](#)]
3. Fernandez-Jimenez, A.; Palomo, A.; Criado, M. Microstructure development of alkali-activated fly ash cement descriptive model. *Cem. Concr. Res.* **2005**, *35*, 1204–1209. [[CrossRef](#)]
4. Park, S.S.; Kang, H.Y. Strength and microscopic characteristics of alkali-activated fly ash-cement. *Korean J. Chem. Eng.* **2006**, *23*, 367–373. [[CrossRef](#)]
5. Fernandez-Jimenez, A.; Garcia-Lodeiro, L.; Palomo, A. Durability of alkali-activated fly ash cementitious materials. *J. Mater. Sci.* **2007**, *42*, 3055–3065. [[CrossRef](#)]
6. Ma, Y.; Hu, J.; Ye, G. The effect of activating solution on the mechanical strength, reaction rate, mineralogy, and microstructure of alkali-activated fly ash. *J. Mater. Sci.* **2012**, *47*, 4568–4578. [[CrossRef](#)]
7. Nath, S.K.; Kumar, S. Influence of iron making slags on strength and microstructure of fly ash geopolymer. *Constr. Build. Mater.* **2013**, *38*, 924–930. [[CrossRef](#)]



8. Rashad, A.M. A comprehensive overview about the influence of different admixtures and additives on the properties of alkali-activated fly ash. *Mater. Design*. **2014**, *53*, 1005–1025. [[CrossRef](#)]
9. Law, D.W.; Adam, A.A.; Molyneaux, T.K.; Patnaikuni, I.; Wardhono, A. Long term durability properties of class F fly ash geopolymer concrete. *Mater. Struct.* **2015**, *48*, 721–731. [[CrossRef](#)]
10. Khan, M.Z.N.; Shaikh, F.U.A.; Hao, Y.F.; Hao, H. Synthesis of high strength ambient cured geopolymer composite by using low calcium fly ash. *Constr. Build. Mater.* **2016**, *125*, 809–820. [[CrossRef](#)]
11. Ding, Y.C.; Cheng, T.W.; Dai, Y.S. Application of geopolymer paste for concrete repair. *Struct. Concrete* **2017**, *18*, 561–570. [[CrossRef](#)]
12. Rakhimova, N.R.; Rakhimov, R.Z. Reaction products, structure and properties of alkali-activated metakaolin cements incorporated with supplementary materials—a review. *J. Mater. Res. Technol.* **2019**, *8*, 1522–1531. [[CrossRef](#)]
13. Katpady, D.N.; Takewaka, K.; Yamaguchi, T.; Akira, Y. Performance of slag based Shirasu geopolymer cured under ambient condition. *Constr. Build. Mater.* **2020**, *234*, 117210. [[CrossRef](#)]
14. Guo, X.L.; Pan, X.J. Effects of steel slag on mechanical properties and mechanism of fly ash-based geopolymer. *J. Mater. Civil. Eng.* **2020**, *32*, 04019348. [[CrossRef](#)]
15. Ng, Y.S.; Liew, Y.M.; Heah, C.Y.; Abdullah, M.M.A.; Chan, L.W.L.; Ng, H.T.; Ong, S.W.; Ooi, W.E.; Hang, Y.J. Evaluation of flexural properties and characterisation of 10-mm thin geopolymer based on fly ash and ladle furnace slag. *J. Mater. Res. Technol.* **2021**, *15*, 163–176.
16. Stankiewicz, N. Effect of Admixtures on Selected Properties of Fly Ash-Based Geopolymer Composites. *Appl. Sci.* **2023**, *13*, 1803. [[CrossRef](#)]
17. Wang, C.H.; Wen, P.H.; Wang, M.H.; Fan, Q.J.; Wang, X.Q. Preparation and characterization of road alkali-activated blast furnace slag paste. *Constr. Build. Mater.* **2018**, *181*, 175–184. [[CrossRef](#)]
18. Xiang, J.C.; Liu, L.P.; Cui, X.M.; He, Y.; Zheng, G.J.; Shi, C.J. Effect of Fuller-fine sand on rheological, drying shrinkage, and microstructural properties of metakaolin-based geopolymer grouting materials. *Cement Concrete Comp.* **2019**, *104*, 103381. [[CrossRef](#)]
19. Liu, F.Q.; Zheng, M.L.; Ye, Y.S. Formulation and properties of a newly developed powder geopolymer grouting material. *Constr. Build. Mater.* **2020**, *258*, 120304. [[CrossRef](#)]
20. Xu, J.; Kang, A.H.; Wu, Z.G.; Xiao, P.; Gong, Y.F. Effect of high-calcium basalt fiber on the workability, mechanical properties and microstructure of slag-fly ash geopolymer grouting material. *Constr. Build. Mater.* **2021**, *302*, 124089. [[CrossRef](#)]
21. Xu, J.; Kang, A.H.; Wu, Z.G.; Xiao, P.; Li, B.; Lu, Y.M. Research on the Formulation and Properties of a High-Performance Geopolymer Grouting Material Based on Slag and Fly Ash. *KSCE J. Civ. Eng.* **2021**, *25*, 3437–3447. [[CrossRef](#)]
22. Zhou, S.Q.; Yang, Z.N.; Zhang, R.R.; Li, F. Preparation, characterization and rheological analysis of eco-friendly road geopolymer grouting materials based on volcanic ash and metakaolin. *J. Clean. Prod.* **2021**, *312*, 127822. [[CrossRef](#)]
23. Zeng, Q.W.; Gao, P.W.; Li, K.; Dong, G.Q.; Jin, G.L.; Sun, X.W.; Zhao, J.W.; Chen, L.F. Experimental Research on the Properties and Formulation of Fly Ash Based Geopolymer Grouting Material. *Buildings* **2022**, *12*, 503. [[CrossRef](#)]
24. Liu, J.W.; Feng, H.; Zhang, Y.X.; Zheng, K.Q. Performance Investigation of Geopolymer Grouting Material with Varied Mix Proportions. *Sustainability* **2022**, *14*, 13046. [[CrossRef](#)]
25. Yue, J.C.; Nie, X.F.; Wang, Z.R.; Liu, J.L.; Huang, Y.C. Research on the Pavement Performance of Slag/Fly Ash-Based Geopolymer-Stabilized Macadam. *Appl. Sci.* **2022**, *12*, 10000. [[CrossRef](#)]
26. Sofri, L.A.; Abdullah, M.M.A.; Sandu, A.V.; Imjai, T.; Vizureanu, P.; Hasan, M.R.M.; Almadani, M.; Ab Aziz, I.H.; Rahman, F.A. Mechanical Performance of Fly Ash Based Geopolymer (FAG) as Road Base Stabilizer. *Materials* **2022**, *15*, 7242. [[CrossRef](#)]
27. Wu, D.Z.; Zhang, Z.L.; Chen, K.Y.; Xia, L.L. Experimental Investigation and Mechanism of Fly Ash/Slag-Based Geopolymer-Stabilized Soft Soil. *Appl. Sci.-Basel.* **2022**, *12*, 7438. [[CrossRef](#)]
28. Li, J.; Dang, X.T.; Zhang, J.W.; Yi, P.; Li, Y.M. Mechanical Properties of Fly Ash-Slag Based Geopolymer for Repair of Road Subgrade Diseases. *Polymers* **2023**, *15*, 309. [[CrossRef](#)]
29. GB/T 18046-2017; Ground Granulated Blast Furnace Slag Used for Cement, Mortar and Concrete. Standards Press of China: Beijing, China, 2017.
30. JTG 3420-2020; Testing Methods of Cement and Concrete for Highway Engineering. China Communications Press: Beijing, China, 2020.

**Disclaimer/Publisher’s Note:** The statements, opinions and data contained in all publications are solely those of the individual author(s) and contributor(s) and not of MDPI and/or the editor(s). MDPI and/or the editor(s) disclaim responsibility for any injury to people or property resulting from any ideas, methods, instructions or products referred to in the content.